ISBN: 978-3-95450-215-8 ISSN: 2226-0366 doi:10.18429/JACoW-LINAC2022-MO1PA02

BEAM COMMISSIONING OF NORMAL CONDUCTING PART AND STATUS OF ESS PROJECT

R. Miyamoto*, C. Amstutz, S. Armanet, R. Baron, E. Bergman, A. Bhattacharyya, B. Bolling, W. Borg, S. Calic, M. Carroll, J. Cereijo Garcia, J. Christensson, J. Christie, H. Danared, C. Derrez, I. Kittelmann, E. Donegani, S. Ekström, M. Eriksson, M. Eshraqi, J. Esteban Müller, K. Falkland, A. Forsat, S. Gabourin, A. Garcia Sosa, A. Gorzawski, S. Grishin, P. Gustavsson, W. Hees, M. Jensen, B. Jones, S. Haghtalab, V. A. Harahap, H. Hassanzadegan, J. Jamroz, A. Jansson, M. Juni Ferreira, M. Kalafatic, H. Kocevar, S. Kövecses, E. Laface, B. Lagoguez, Y. Levinsen, M. Lindroos, A. Lundmark, M. Mansouri, C. Marrelli, C. Martins, J. Martins, S. Micic, N. Milas, M. Mohammednezhad, R. Montano, M. Munoz, G. Mörk, D. Nicosia, B. Nilsson, D. Noll, A. Nordt, T. Olsson, N. Öst, L. Page, D. Paulic, S. Pavinato, A. Petrushenko, C. Plostinar, J. Riegert, A. Rizzo, K. Rosengren, K. Rosquist, M. Serluca, T. Shea, A. Simelio, S. Slettebak, H. Spoelstra, A. Svensson, L. Svensson, R. Tarkeshian, L. Tchelidze, C. Thomas, E. Trachanas, P. van Velze, K. Vestin, R. Zeng, ESS, Lund, Sweden
A. C. Chauveau, P. Hamel, O. Piquet, CEA, Saclay, France
I. Bustinduy, A. Conde, D. Fernandez-Cañoto, N. Garmendia, P. J. Gonzalez, G. Harper, A. Kaftoosian, J. Martin, I. Mazkiaran, J. L. Munoz, A. R. Páramo, S. Varnasseri, A. Zugazaga, ESS-Bilbao, Bilbao, Spain
C. Baltador, L. Bellan, M. Comunian, F. Grespan, A. Pisent, INFN, Italy

Abstract

The European Spallation Source, currently under construction in Lund Sweden, will be a spallation neutron source driven by a superconducting proton linac with a design power of 5 MW. The linac features a high peak current of 62.5 mA and long pulse length of 2.86 ms with a repetition rate of 14 Hz. The normal conducting part of the linac has been undergoing beam commissioning in multiple steps, and the main focus of the beam commissioning has been on bringing systems into operation, including auxiliary ones. In 2022, beam was transported to the end of the first tank of the five-tank drift tube linac. This paper provides a summary of the beam commissioning activities at ESS and the current status of the linac.

INTRODUCTION

European Spallation Source (ESS) [1], currently under construction in Lund, Sweden, is a neutron source driven by a superconducting (SC) proton linac with a design beam power of 5 MW. When the beam power exceeds 2 MW, the ESS will the brightest neutron source in the world. The linac has a normal-conducting injector, consisting of an ion source (IS), low energy beam transport (LEBT), radio-frequency quadrupole (RFQ), medium energy beam transport (MEBT), and drift-tube linac (DTL) with five tanks. The SC part uses three types of cavities: spoke cavities, medium-β elliptical cavities, and high-β elliptical cavities. Following the SC part is the high energy beam transport (HEBT), which has rooms for additional cryomodules (up to 16) as contingency or for potential upgrades. After the HEBT, the linac is split into two: a straight transport line to the tuning beam dump and a dogleg with a 4 degrees bend and 4.5 m elevation. The section after the dogleg is referred to as Accelerator-to-Target (A2T), where each beam pulse is painted over the spallation target with a cross-check pattern and rectangular border by using the rastering system [2, 3]. In the following, the part from the IS to DTL is referred to as the normal-conducting linac (NCL), and the rest is referred to as the superconducting linac (SCL). Figure 1 shows a schematics layout of the linac, and Table 1 lists the high-level parameters for the design [1] and during the initial operations [4]. The design energy of 2 GeV, with a 62.5 mA current and 4% duty factor, makes a 5 MW beam power. The beam energy will be limited to 800 MeV during the initial operations due to a budget issue, and this reduces the beam power to 2 MW.

Table 1: ESS Linac High Level Parameters for the Design and Initial Operations (Ops.)

Parameter	Unit	Value
Beam power (design)	MW	5
Beam energy (design)	GeV	2
Beam power (initial Ops.)	MW	5
Beam energy (initial Ops.)	GeV	0.8
Peak beam current	mA	62.5
Beam pulse length	ms	2.86
Beam pulse repetition rate	Hz	14
Duty factor	%	4
RF frequency	MHz	352.21/704.42
Availability	%	95

* ryoichi.miyamoto@ess.eu

ISBN: 978-3-95450-215-8 ISSN: 2226-0366 doi:10.18429/JACoW-LINAC2022-MO1PA02

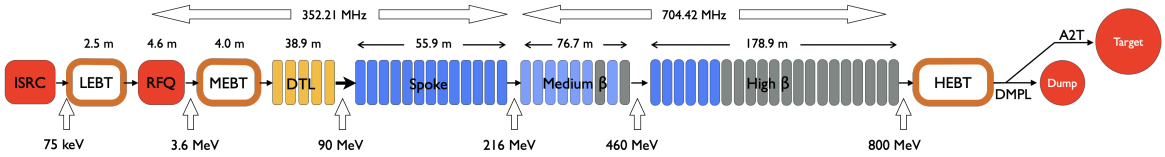

Figure 1: ESS linac schematic layout for the initial operations with 800 MeV and 2 MW. The segments in the DTL and SC sections denote a DTL tank or a cryomodule. The cryomodules marked with the grey color will not be powered during the initial 2 MW operations.

The long pulse length of 2.86 ms is a requirement from the users and unique feature of the ESS. The ESS also has an ambitious goal of high availability of 95%.

The NCL of the ESS linac already went through three commissioning steps, and the nominal current beam was successfully sent through the first DTL tank (DTL1). For the rest of the linac, manufacturing, installation, and testing of components are ongoing. This paper first provide a brief summary on the ESS linac project and then presents a summary and highlights of the NCL commissioning activities on the ESS site.

PROJECT STATUS

This section provides a brief overview on the whole ESS linac project. Further details can be found in [4, 5].

Schedule and Linac Configurations

The ESS follows a strategy of staged commissioning like other similar facilities. For each commissioning step and the start of the user operations, the starting time and the maximum energy at that time are summarized in Table 2. As denoted in Fig. 1, the number of cryomodules for the spokes, medium-β, and high-β cavities are 13, 9, and 21 for each. Each spoke cryomodules houses two spoke cavities whereas each medium- and high-β cryomodule houses four cavities. From the early years of the project, it has been planned that the high-β cryomodules are not installed for the fifth and sixth commissioning steps in Table 2 [6]. This is why the maximum energy for those steps is 570 MeV, which is the design energy after the medium-β section. The current plan is slightly different and assumes seven medium-β cryomodules (the blue color ones in Fig. 1) and two high-β cryomodules for those steps [4]. This is due to production issues with the medium-β cavities and good progress with production of high-β cryomodules. This configuration also gives the maximum energy of approximately 570 MeV. The remaining two medium-β and 19 high-β cryomodules will be installed later, but only five of them (and in total seven) are powered, thus making the beam energy during the initial operations 800 MeV.

Table 2: ESS Linac High-level Schedule

Step	Start	Energy [MeV]
Commissioning to LEBT	2018-09	0.075
Commissioning to MEBT	2021-11	3.62
Commissioning to DTL1	2022-05	21
Commissioning to DTL4	2023	74
Commissioning to Dump	2024	570
Commissioning to Target	2025	570
Start of user operations	2026	800

Recent Highlights on the ESS Site

Overall, the ESS linac project is making steady progress towards the major milestones of the first beam on target and initial user operations. Because it is a European collaboration with more than 20 institutions, there is not enough space to list progresses in all areas. Thus, this section lists highlights only from recent activities on the ESS site. Currently, the accelerator tunnel is separated by a temporary shield wall at the foreseen location of DTL5. This is to allow activities such as high-power conditioning of cavities and beam commissioning in the NCL side in parallel to installation and testing in the SCL side.

For the NCL, besides the beam commissioning, high-power conditioning of the RFQ and DTL1 was successfully conducted on the ESS site. The RFQ reached steady operations at 850 kW (116% of the nominal power) for the full duty factor. Whereas, for the DTL1, time ran out after reaching steady operations at 3.15 MV/m (105% of the nominal field) for 14 Hz but for a ~1 ms pulse length. Details on the experiences from the RFQ and DTL1 conditioning were presented in this conference [7, 8].

For the SCL, the cryomodules are being delivered to the ESS. So far, the number of the received cryomodules for the spoke, medium-β, and high-β cavities are eight, seven, and two for each, *i.e.*, what is missing for the fifth and sixth commissioning steps is five spoke cryomodules. In the SCL side of the tunnel, installation of the cryogenic distribution was just completed. Once its testing is completed, installation of the cryomodules is scheduled to start in 2023. Details of cryomodule production, testing, and installation were presented in this conference [9]. Installation and testing of the RF systems for the cryomodules are also progressing in the gallery.

NCL COMMISSIONING OVERVIEW

NCL Structures

This section provides short descriptions of the NCL structures up to DTL1. Further details can be found in [1, 5].

ISBN: 978-3-95450-215-8 ISSN: 2226-0366 doi:10.18429/JACoW-LINAC2022-MO1PA02

The IS of the ESS is of the microwave discharge type and produces a 75 keV proton beam. The following LEBT has two focusing solenoids equipped with coils for trajectory correction. The LEBT includes the following diagnostics [10]: Faraday cup (FC), beam current monitor (BCM), Doppler detector for a proton fraction measurement, Allison scanner type emittance measurement units (EMUs), and non-invasive profile monitors (NPMs), which also provide a centroid position measurement. Figure 2 is a schematic layout of the LEBT. Note that there is an additional BCM around the cable of the 75 kV high-voltage power-supply, which provides an indirect measurement of the current out of the IS. During the first commissioning step for the IS and LEBT, and also during the preceding commissioning at the site of the INFN-LNS [11], an additional tank was placed at the position of the RFQ, and the second set of the NPMs and one of the EMU were placed in this tank.

After the LEBT, a 4.6 m-long, four-vane RFQ accelerates the proton beam to 3.62 MeV and forms the bunch structure of 352.21 MHz. The subsequent 4 m-long MEBT includes three buncher cavities and eleven quadrupoles equipped with coils for dipole correctors. The MEBT houses a comprehensive set of diagnostics: FC, BCMs, beam position monitors (BPMs) both for position and phase measurements, wire-scanners (WSs), slit and grid type EMU, and bunch shape monitor for longitudinal profile measurements. Figure 3 is a schematic layout of the MEBT. Note that the FC is in front of the eighth quadrupole and this FC was final destination during the second commissioning step.

The DTL1 with 61 acceleration gaps accelerates beam from 3.62 MeV to 21 MeV. Every other drift-tube houses a permanent magnet quadrupole (PMQ), forming the FODO lattice for transverse focusing. DTL1 also houses six dipole correctors and six BPMs in drift-tubes with no PMQ. During the third commissioning step, an FC was placed after the DTL1 with a ~1 m drift and shielding.

The beam pulse out of the IS is much longer than the nominal 2.86 ms (~6 ms) because of the stabilization time of a few milliseconds in the beginning. Adjustments of the pulse length and cleaning of the edges are performed with the slow and fast choppers housed in the LEBT and MEBT, respectively. Adjustments of the current is performed with the IS itself and the iris in the LEBT.

Strategy and Constraints

The ESS linac project has been adopting aggressive schedule since the beginning, which lead to the decision of not

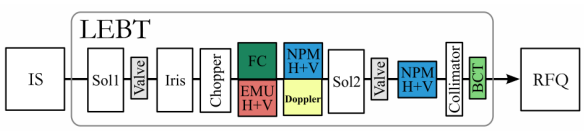

Figure 2: LEBT schematic layout during operations. During the commissioning for the IS and LEBT, an additional tank was placed at the position of the RFQ.

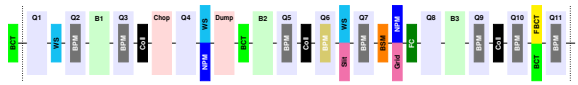

Figure 3: MEBT schematic layout.

using any temporary test-bench or beam dump after the commissioning step for the IS and LEBT [6] but instead including comprehensive suite of permanent diagnostics in the linac [12]. The choice of no temporary beam dump defined relatively tight limits in beam parameters during the NCL commissioning (except when the beam is sent to the LEBT FC): 62.5 mA and 50 µs for 1 Hz and 62.5 mA and 5 µs for 14 Hz. Testing a duty factor higher than these sets of parameters has to be waited until the beam is sent to the tuning beam dump, which is still limited to only 1/30 Hz for the full nominal pulse. The aggressive schedule, combined with limited resource for systems integration to the control system, also lead to the situation where each commissioning step thus far started with the minimal set of systems, especially for the diagnostics. When the first commissioning step for the IS and LEBT started, only the BCMs and FC were available. The NPMs and EMUs later received temporary integration and provided measurement results during this commissioning steps. However, because of their temporary status, they became unavailable again during the following commissioning steps. Similarly, for the second and third steps of commissioning, only the FCs, BCMs, and BPMs were available from the beginning. The WSs and EMUs in the MEBT were later tested with beam but provided only limited sets of measurements. In terms of cavities and their RF systems, the buncher cavities were not available during the whole period of the commissioning to MEBT in 2021 since their RF systems were not deployed yet at that point. The feedback and adaptive feed-forward of the low-level RF (LLRF) systems were still under testing phases for all the cavities.

Because of the above-mentioned situations, for the second and third commissioning steps, priority was given for deploying and verifying as many systems as possible. In terms of beam parameters, the baseline goal was set very low to establish stable probe beam (≤6 mA, 5 µs, and 1 Hz) to the final destination of the given step.

Highlights

The initial part of the second commissioning step took a very cautious approach prior to sending the beam to the RFQ and ramping up beam parameters and spent time for verifying the systems critical for machine safety such as the BCMs, LEBT chopper, and machine protection systems [13]. Nevertheless, within the allocated period of five weeks in 2021, the beam was successfully accelerated with the RFQ and stable beam with 6 mA, 50 µs, and 1 Hz was established up to the MEBT FC, without any accident. The output energy of the RFQ was verified to be ~3.6 MeV with time-of-flight measurements (Fig. 4). In 2022, two additional commissioning periods (approximately nine weeks in total)

ISBN: 978-3-95450-215-8 ISSN: 2226-0366 doi:10.18429/JACoW-LINAC2022-MO1PA02

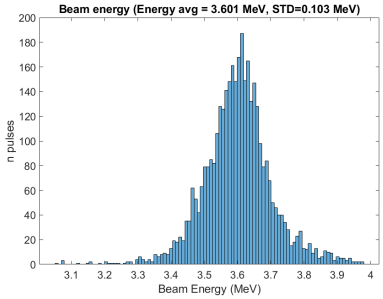

Figure 4: Histogram of the measured RFQ energy with time-of-flight.

Table 3: NCL Commissioning Milestones

Milestone	Date
Beam from IS	2018-09-19
Acceleration with RFQ	2021-11-26
Nominal current out of RFQ	2022-03-12
Acceleration with DTL1	2022-06-01
Nominal current out of DTL1	2022-07-01

were arranged. During these periods, stable beam with the nominal 62.5 mA current was established up to the MEBT FC, with an excellent RFQ transmission of ~95%. Testing of the closed-loop operation of the RFQ also made good progress during this period, and the RFQ ran with both the feedback and adaptive feed-forward during the following commissioning step.

During the following commissioning step up to the DTL1, it did not take too long to send the beam to the DTL1 and attempt to ramp-up the current. This was because most of the critical systems for machine safety were already verified during the preceding step. Transport beam with the nominal 62.5 mA current was first attempted on 1st of July, 2022 and established within a few hours. Table 3 lists selected milestones from the second and third commissioning steps.

HIGHLIGHTS FROM BEAM CHARACTERIZATION AND TUNING

This section presents selected highlights of beam characterizations and tuning from the NCL commissioning steps thus far. Further details could be found in the contributions to this conference [7, 14–18] as well as in the upcoming conference of this year (2022) [19, 20].

IS Repeller

During a maintenance period in early 2022, it was discovered that the repeller located ~30 mm from the extraction hole was disconnected. This repeller prevents electrons from back-streaming into the IS chamber from the LEBT. It also changes the balance between the electric potentials of the extraction system and beam space-charge and thus potentially alters beam characteristics [16]. The first commissioning step for the IS and LEBT showed large emittance values (0.3-0.4 π mm mrad depending on the extracted current) and

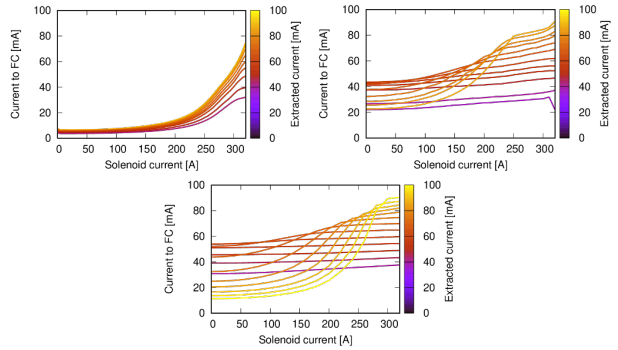

Figure 5: Transmission to the LEBT FC for various extraction current levels and first solenoid strengths, before (top-left) and after (top-right) the discovery of the IS repeller issue, compared to the model prediction (bottom).

indicated a large initial divergence [21]. Transmission measurements up to the LEBT FC for different levels of the extraction current and strength of the first solenoid (Figure 5) confirmed that the repeller was the cause of this issue. The initial divergence is clearly reduced with the repeller (thus improving the transmission in the low solenoid strength region) and the measurements show much better agreement to the model prediction. A further, detailed analysis of the effect of this repeller can be seen in [16].

Matching to RFQ

Matching from the LEBT to RFQ was performed by scanning two solenoids in the LEBT and finding the combination which maximizes the transmission through the RFQ. Like many other RFQs, this condition is also the best for beam quality, *e.g.*, minimizing emittance growth in all the planes [22]. Figure 6 compares a measurement (left) and simulations (middle and right), which are based on three codes: IBSimu [23] for the IS output distribution, TraceWin [24] for the transport in the LEBT, and Toutatis [25] for the transport in the RFQ. The condition of the simulations needs to be improved, for example the maximum current into the RFQ was ~62 mA for the measurement whereas ~69 mA for the simulations. The best transmission measured was 95.5%, which was very close to the model prediction of 97-98%. On the other hand, the position of the optimal point and the pattern were quite different. It is also seen that the simulation result is sensitive against the level of space-charge compensation (SCC). These results are still preliminary; additional measurements will be performed in future and simulation studies will continue.

For the injection to the RFQ, correcting the trajectory error is also important. During the first commissioning step, trajectory correction and error source identifications were made based on position measurements from the NPMs [26, 27]. The significance of the Earth magnetic field, which had a downward vertical component of 47.4 µT [28], was also identified. Because the NPMs were not available, stability of the trajectory correction could not be tested during the second and third commissioning steps. During the second

ISBN: 978-3-95450-215-8 ISSN: 2226-0366 doi:10.18429/JACoW-LINAC2022-MO1PA02

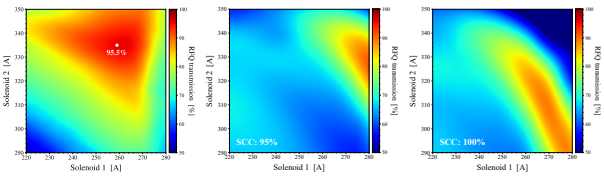

Figure 6: RFQ transmission vs. LEBT solenoids. Left: Measurement. Middle: simulations with 95% SCC. Right: Simulation with 100% SCC. (For the solenoid, the conversion from current to peak field is 0.8158 mT/A.)

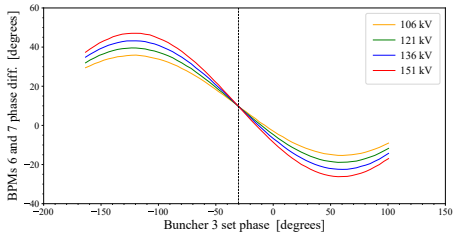

Figure 7: BPM phase difference between two downstream BPMs during the buncher 3 phase scan. The different colors are for different set effective voltages (VT).

step of commissioning, another scheme to correct the positions at the RFQ injection was also established by using the BPMs in the MEBT and combining scans of the correctors with modulation of the RFQ voltage [17].

RF Phase and Amplitude Setting

Beyond the RFQ, the most significant part of hadron linac tuning, especially in the beginning, is to set the RF amplitudes and phases of all the RF cavities one-by-one from the downstream, and thus establishing synchronizations among cavities and intended energy at each point. This is typically done by scanning the phase of the cavity under tuning for different levels of amplitudes, while all the other downstream cavities are turned off, and by measuring the phases changes in downstream locations. Details of the RF tuning conducted so far will be presented in [20].

Figure 7 shows an example of such scans for the third buncher. All the curves cross a point at a −30 degrees in phase, where the buncher causes no acceleration and only providing bunching. The amplitude of the oscillation is proportional to the cavity voltage (V) multiplied by the transit-time-factor (T). Hence, a comparison of the amplitude to the model gives beam-based calibration to the cavity amplitude. In this case, it was found that the set amplitude was off by approximately −10%.

The amplitude and phase of each DTL tank can be also set in a similar manner based on phase measurement. For a DTL tank, the phase signal tends to be more complex than the case of the bunchers and the curve fitting is used to determine the amplitude and phase (*signature matching*) [29]. For the DTL of the ESS linac, applying machine-learning technique was also studied for future applications [30]. For the DTL1, the amplitude and phase can be also set roughly with transmission scan like the RFQ. This is because no beam comes out of it for a certain range of phase, even if its amplitude is at the design value. This is not the case for the rest of the tanks of the ESS DTL. Figure 8-left shows the DTL1 transmission scanned over the phase for different levels of amplitudes. The transmission was measured between the BCM the end of the MEBT and the other at the end of the DTL1. The shoulders of these transmission curves depend on the bunch length in time at the DTL1 entrance, whereas the full-width-half-maximum (FWHM) of each curve is insensitive against the initial bunch length and thus is a good figure of merit. Figure 8-right shows the relation between the FWHM and the set amplitude, where the FWHM was calculated by fitting an error function to each shoulder. The horizontal axis is the relative amplitude, whose reference was adjusted so that the measured data points fit to the simulation. This preliminary analysis indicated that the set voltage of 2.9 MV/m was closest to the nominal field case of the simulation. The design phase is ∼70 degrees from the half-crossing of the right shoulder (and ∼40 degrees from the left), which is at ∼130 degrees in the left figure.

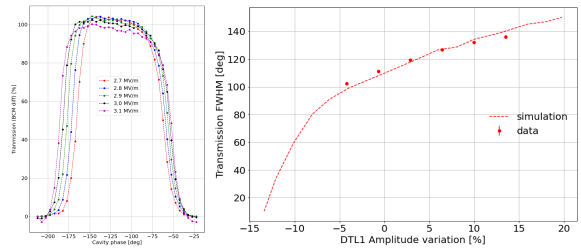

Figure 8: Left: DTL1 transmission vs. phase. Right: FWHM vs. amplitude. In the right figure, the reference of the relative amplitude (horizontal axis) was selected so that the measurement points overlap with the model prediction, indicating that the set amplitude of 2.9 MV/m is closest to provide the nominal 3.0 MV/m field.

CONCLUSIONS

The ESS linac project is making a steady progress towards the initial operation at 800 MeV and 2 MW. For the NCL, the commissioning step up to DTl1 was just completed. Despite that only the fundamental diagnostics of FCs, BCMs, and BPM was available for a large fraction of commissioning time, the nominal current beam with 62.5 mA was successfully transported to the end of DTL1 on the day of the first attempt. Three additional DTL tanks will be installed and go through high-power conditioning this year (2022), followed by beam commissioning next year. For the SCL, the cryomodules are being delivered and tested. Their installation will start next year, aiming to conduct the beam commissioning of the SCL in 2024.

ACKNOWLEDGEMENTS

The authors would like to thank all the other contributors to the ESS linac project, not listed in the author list.

ISBN: 978-3-95450-215-8 ISSN: 2226-0366 doi:10.18429/JACoW-LINAC2022-MO1PA02

REFERENCES

[1] R. Garoby *et al.*, "The European Spallation Source Design," *Physica Scripta*, vol. 93, no. 1, p. 014 001, 2017. doi:10.1088/1402-4896/aa9bff

[2] H. Thomsen and S. Møller, "The Design of the Fast Raster System for the European Spallation Source," in *Proc. 5th International Particle Accelerator Conference (IPAC'14)*, Dresden, Germany, 2014, pp. 2118–2120. doi:10.18429/JACoW-IPAC2014-WEPRO072

[3] H. Thomsen and S. Møller, "The ESS High Energy Beam Transport after the 2013 Design Update," in *Proc. 5th International Particle Accelerator Conference (IPAC'14)*, Dresden, Germany, 2014, pp. 2121–2123. doi:10.18429/JACoW-IPAC2014-WEPRO073

[4] A. Jansson, "The Status of the ESS Project," in *Proc. 13th International Particle Accelerator Conference (IPAC'22)*, Bangkok, Thailand, 2022, paper TUIYGD1, pp. 792–795. doi:10.18429/JACoW-IPAC2022-TUIYGD1

[5] D. Plostinar *et al.*, "Status of the Normal Conducting Linac at the European Spallation Source," in *Proc. 13th International Particle Accelerator Conference (IPAC'22)*, Bangkok, Thailand, 2022, paper WEPOTK001, pp. 2019–2022. doi:10.18429/JACoW-IPAC2022-WEPOTK001

[6] R. Miyamoto, M. Eshraqi, and M. Muñoz, "ESS Linac Plans for Commissioning and Initial Operations," in *Proc. of ICFA Advanced Beam Dynamics Workshop on High-Intensity and High-Brightness Hadron Beams (HB'16)*, Malmö, Sweden, 2016, pp. 342–347. doi:10.18429/JACoW-HB2016-TUPM5Y01

[7] R. Zeng and O. Piquet, "RFQ Performance During RF Conditioning and Beam Commissioning at ESS," in *Proc. 31st Linear Accelerator Conference (LINAC'22)*, 2022, paper TUPOPA05.

[8] F. Grespan *et al.*, "High Power RF Conditioning of the ESS DTL1," in *Proc. 31st Linear Accelerator Conference (LINAC'22)*, 2022, paper TUPOJO09.

[9] C. G. Maiano, "Production, Tests and Installation of the ESS Spoke, Medium and High Beta Cryomodules," in *Proc. 31st Linear Accelerator Conference (LINAC'22)*, 2022, paper TH1PA02.

[10] C. Derrez *et al.*, "Initial Performance of the Beam Instrumentation for the ESS IS & LEBT," in *Proc. 10th International Particle Accelerator Conference (IPAC'19)*, Melbourne, Australia, 2019, pp. 2650–2653. doi:10.18429/JACoW-IPAC2019-WEPGW076

[11] Ø. Midttun, "Off-site commissioning report for the ESS proton source and LEBT," ESS, Tech. Rep. ESS-0190279, 2018.

[12] T. Shea *et al.*, "Overview and Status of Diagnostics for the ESS Project," in *Proc. of International Beam Instrumentation Conference (IBIC'17)*, Grand Rapids, MI, USA, 2018, pp. 8–15. doi:10.18429/JACoW-IBIC2017-MO2AB2

[13] S. Gabourin, M. Carroll, S. K. de Carvalho, A. Nordt, S. Pavinato, and K. Rosquist, "The ESS Fast Beam Interlock System: First Experience of Operating With Proton Beam," in *Proc. 31st Linear Accelerator Conference (LINAC'22)*, 2022, paper MOPORI17.

[14] B. Jones *et al.*, "Hardware Commissioning With Beam at the European Spallation Source: Ion Source to DTL1," in *Proc. 31st Linear Accelerator Conference (LINAC'22)*, 2022, paper TUPOJO10.

[15] L. Neri *et al.*, "HSMDIS Performance on the ESS Ion Source," in *Proc. 31st Linear Accelerator Conference (LINAC'22)*, 2022, paper THPORI19.

[16] L. Bellan *et al.*, "Space Charge and Electron Confinement in High Current Low Energy Transport Lines: Experience and Simulations From IFMIF/EVEDA and ESS," in *Proc. 31st Linear Accelerator Conference (LINAC'22)*, 2022, paper TUPORI29.

[17] D. Noll *et al.*, "First Beam Matching and Transmission Studies on the ESS RFQ," in *Proc. 31st Linear Accelerator Conference (LINAC'22)*, 2022, paper TUPOPA04.

[18] A. G. Sosa *et al.*, "Status of Testing and Commissioning of the Medium Energy Beam Transport Line of the ESS Normal Conducting Linac," in *Proc. 31st Linear Accelerator Conference (LINAC'22)*, 2022, paper TUPOJO14.

[19] N. Milas, A. A. Gorzawski, and J. J. Jamroz, "Commissioning of the Timing System at ESS," in *Proc. 11th International Beam Instrumentation Conference (IBIC'22)*, 2022.

[20] Y. Levinsen *et al.*, "First RF Phase Scans in the European Spallation Source," in *Proc. 11th International Beam Instrumentation Conference (IBIC'22)*, 2022.

[21] R. Miyamoto *et al.*, "First Results of Beam Commissioning on the ESS Site for the Ion Source and Low Energy Beam Transport," in *Proc. 10th International Particle Accelerator Conference (IPAC'19)*, Melbourne, Australia, 2019, pp. 1118–1121. doi:10.18429/JACoW-IPAC2019-MOPTS103

[22] R. Miyamoto *et al.*, "Preparation Towards the Ess Linac Ion Source and Lebt Beam Commissioning on Ess Site," in *Proc. 9th International Particle Accelerator Conference (IPAC'18)*, Vancouver, BC, Canada, 2018, pp. 874–877. doi:10.18429/JACoW-IPAC2018-TUPAF064

[23] T. Kalvas *et al.*, "IBSIMU: A three-dimensional simulation software for charged particle optics," *Review of Scientific Instruments*, vol. 81, 02B703, 2010.

[24] D. Uriot and N. Pichoff, "Status of TraceWin Code," in *Proc. 6th International Particle Accelerator Conference (IPAC'15)*, Richmond, VA, USA, 2015, pp. 92–94. doi:10.18429/JACoW-IPAC2015-MOPWA008

[25] R. Duperrier, "TOUTATIS: A radio frequency quadrupole code," *Phys. Rev. ST Accel. Beams*, vol. 3, p. 124 201, 2000. https://journals.aps.org/prab/abstract/10.1103/PhysRevSTAB.3.124201

[26] E. Nilsson, M. Eshraqi, J. E. Müller, Y. Levinsen, N. Milas, and R. Miyamoto, "Beam Dynamics Simulation with an Updated Model for the ESS Ion Source and Low Energy Beam Transport," in *Proc. 10th International Particle Accelerator Conference (IPAC'19)*, Melbourne, Australia, 2019, pp. 1042–1045. doi:10.18429/JACoW-IPAC2019-MOPTS083

[27] N. Milas *et al.*, "Beam Based Alignment of Elements and Source at the ESS Low Energy Beam Transport Line," in *Proc. 8th International Beam Instrumentation Conference(IBIC'19)*, Malmö, Sweden, 2019, pp. 600–604. doi:10.18429/JACoW-IBIC2019-WEPP032

ISBN: 978-3-95450-215-8 ISSN: 2226-0366 doi:10.18429/JACoW-LINAC2022-MO1PA02

[28] http://www.geomag.bgs.ac.uk

[29] M. Comunian, L. Bellan, M. Eshraqi, F. Grespan, R. Miyamoto, and A. Pisent, "Commissioning Plans for the ESS DTL," in *Proc. of Linear Accelerator Conference (LINAC'16)*, East Lansing, MI, USA, 2017, pp. 264–266. doi:10.18429/JACoW-LINAC2016-MOPLR059

[30] J. Lundquist, N. Milas, E. Nilsson, and S. Werin, "ESS DTL Tuning Using Machine Learning Methods," in *Proc. 12th International Particle Accelerator Conference (IPAC'21)*, Campinas, SP, Brazil, 2021, paper TUPAB198, pp. 1872–1875. doi:10.18429/JACoW-IPAC2021-TUPAB198